2013

Discrete Particle Modeling of a Novel Prismatic Spouted Bed Reactor

Vitalij Salikov
Hamburg University of Technology, Germany

Vinayak S. Sutkar
Eindhoven University of Technology, Netherlands

Sergiy Antonyuk
Hamburg University of Technology, Germany

Stefan Heinrich
Hamburg University of Technology, Germany

Niels G. Deen
Eindhoven University of Technology, Netherlands

See next page for additional authors

Authors
Vitalij Salikov, Vinayak S. Sutkar, Sergiy Antonyuk, Stefan Heinrich, Niels G. Deen, and Johannes A.M. Kuipers

DISCRETE PARTICLE MODELING OF A NOVEL PRISMATIC SPOUTED BED REACTOR

Vitalij Salikov[1]*, Vinayak S. Sutkar[2], Sergiy Antonyuk[1], Stefan Heinrich[1],
Niels G. Deen[2] and Johannes A.M. Kuipers[2]
1 Hamburg University of Technology, Solids Process Engineering and Particle Technology, Denickestr. 15, 21073 Hamburg, Germany
2 Eindhoven University of Technology; Chemical Engineering and Chemistry Dept.
PO Box 513, 5600 MB Eindhoven, The Netherlands
T: +49-040-42-878-2811; F: +49-040-42-878-2678; E: vitalij.salikov@tuhh.de

ABSTRACT

The goal of this work is the characterization of a novel rectangular (prismatic) spouted bed apparatus with two adjustable gas inlets. In this contribution, the apparatus was modelled using the Discrete Particle Method. The simulations showed a very good agreement with experiments regarding the patterns of granular flow, the bed height and the frequency of pressure fluctuations.

INTRODUCTION

Spouted beds show characteristic circulating patterns of the particle motion. The granular flow here is not rather stochastic as in a fluidized bed, but two distinct regions of an ordered particle flow exist: an upwards directed dilute spout and a dense annulus region, where the particles flow downwards under influence of the gravity (Fig. 1a).

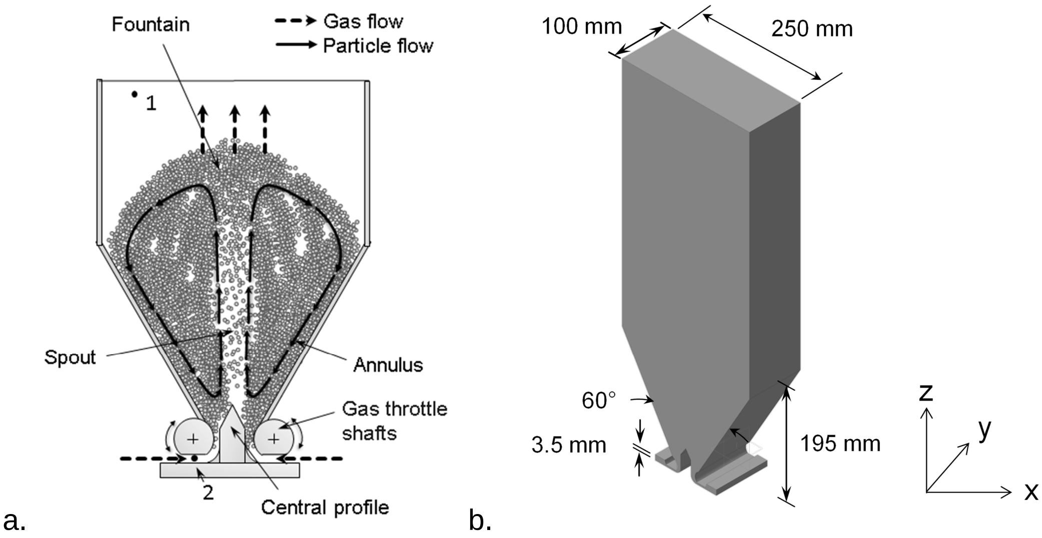

Figure 1: The novel prismatic spouted bed: (a) schematic, (b) modelled interior apparatus volume.

Several research groups modelled spouted beds in 2D and 3D using the coupled Computational Fluid Dynamics (CFD) and Discrete Element Model (DEM), often named as Discrete Particle Method (DPM) (1-5). In (6) we report a DPM study on a shallow prismatic spouted bed at high gas velocities. Several process and geometric parameters, such as the gas flow rate, the angle of the prismatic region and frictional properties of the solids, were varied. All investigated parameters were found to have an influence on the spouting stability, which is in a qualitative agreement with experimental investigations, reported for spouted beds of diverse types. In this contribution, a higher particle bed und more dense granular flow was modelled by an increasing of the bed mass (0.75 vs. 0.5 kg) and a twofold decreasing of the apparatus thickness. The resulting reactor is identical to this recently introduced in (7). This apparatus affiliates with the family of the slot-rectangular spouted beds, which are the subject of considerable academic and industrial research with respect to overcoming the scale-up problem of the conventional axisymmetric reactors. Some investigations are summarized in (8). The specific feature of the modelled novel apparatus is the design of the gas inlet. This is implemented as two horizontal slits and the gas is deflected in the vertical direction by a central profile (Fig. 1a). The slits' height and thus the gas inlet area can be adjusted (also during the operation) by rotation of gas throttle shafts. The gas is sucked through the reactor by a fan. At the modelled higher bed mass and used intermediate gas flow rates, the pressure in the apparatus fluctuates strongly, which allows an analysis of the operational regime using the Fourier-Transformation of the pressure signal, as applied e.g. by Gryczka *et al.* for this type of apparatus (7) and Freitas *et al.* for a rectangular bed with one vertical slot (9). To evaluate the simulation results regarding to the flow patterns, bed height and the pressure fluctuations, the apparatus was constructed with transparent polycarbonate.

METHODS

The spouted bed in general poses an challenge in achieving of a stable spouting using DPM, as pointed out by Takeushi *et al*, regardless of adjustment of the related parameters (2,10). To resolve the gas dynamics in the spout and particularly in the gas inlets' area of a complex geometry, a sufficiently fine computational mesh is required. However, a fine mesh can cause numerical instabilities in CFD solver, if a particle approaches the cell volume and cells can thus be completely occupied by particles (11). However, since usually no particles reside in the inlet area with the highest gas velocity gradients, we encounter the problem using a gradually increasing mesh size, beginning by finer cells in the inlet region. Because of the complex geometry an unstructured computational grid was used. Although, the turbulence is quite strong dampened by particles (11), the introduction of a turbulence model is appropriate for a more accurate solution for areas with a low particle concentration. The κ-ε-model with the renormalization group (RNG) (12) was used because of the high curvature of the gas inlets. Furthermore, the used drag model can have a considerable influence on the simulated spouting, as shown by Gryczka *et al.* by a 2D and 3D two-fluid CFD modelling of this apparatus (13,14); several drag models were tested to study the influence on the simulated spouting patterns and pressure fluctuations. However, irrespective an used model both unrealistic patterns and no regular pressure fluctuations or the strongly underpredicted bed expansion and particle velocities were obtained. It was pointed out, that the choice of an appropriate drag model alone is not sufficient to simulate realistic flow structures and e.g. particle rotation should be considered. In this simulations, we used the combined Ergun - Wen & Yu equations (15,16) as proposed by Gidaspow (17), but resolved the granular flow by the DEM. For the experimental work and the simulation evaluations, a transparent (polycarbonate Europlex® SDX, Evonik, Germany) apparatus was installed. Air is sucked through the apparatus by an exhaust fan. The air throughput was calculated from air velocity in the connecting pipe between the apparatus and the fan, which was measured by using an anemometer (EE65, E+E Elektronik, Austria). Pressure drop was measured by means of a high-speed sensor (differential pressure detector PD-23/8666.1, Testo, Germany). The pressure sensor was connected to a signal convertor and a data acquisition system and analysed using the FFT algorithm in Matlab. Near monosized spherical γ-Al_2O_3-particles (Sasol, Germany) of $d_{50,3}$ = 1.8 mm and density of 1.04 g/cm^3 were used in experiments and simulations. An overview of used parameters and settings can be found in table 1.

Table 1: Parameters and numerical settings

Parameter	**Symbol**	**Value**	**Units**
Edge length of CFD cells (tetrahedral)	-	3.5-20	mm
CFD cell number	N_{cell}	37,220	-
Number of particles	N_P	235,340	-
Bed mass	m_b	750	g
Particle diameter	d_p	1.8	mm
Air flow rate	$\dot{V}$	84; 116	m^3/h
Particle density	ρ_p	1.04	g/cm^3
Restitution coefficient:	e		
particle-particle		0.75	-
particle-wall		0.9	-
Shear modulus:	G		
particles		$5.8\cdot10^9$	Pa
wall		10^9	Pa
Poisson's ratio	ν		
particle		0.25	-
wall		0.25	-
Static friction	μ_s		
particle-particle		0.5	-
particle-wall		0.24	-
Rolling friction	μ_r		
particle-particle		0.05	-
particle-wall		0.06	-
Time step	Δt		
CFD		$5\cdot10^{-5}$ - 10^{-4}	sec.
DEM		$2.5\cdot10^{-7}$	sec.

DPM simulations were performed using commercial codes ANSYS Fluent® and EDEM® in a two-way coupling, which means, that both continuous and discrete phases affect each other. The fluid dynamics are calculated using volume-averaged Navier-Stokes equations:

$$\frac{\partial}{\partial t}\left(\varepsilon\rho_g\right)+\nabla\cdot\left(\varepsilon\rho_g\vec{u}_g\right)=0 \qquad (1)$$

$$\frac{\partial}{\partial t}\left(\varepsilon\rho_g\vec{u}_g\right)+\nabla\cdot\left(\varepsilon\rho_g\vec{u}_g\vec{u}_g\right)=-\varepsilon\,\nabla\cdot p_g-\nabla\cdot\left(\varepsilon\,\vec{\vec{\tau}}_g\right)-\vec{S}_p+\varepsilon\rho_g\vec{g}\,, \qquad (2)$$

Additionally to the coupling by the porosity ε in Eqs. 1 and 2, the influence of particles on the gas momentum (eq. 2) is considered by a sink term:

$$\vec{S}_p = \frac{1}{V_{cell}} \int_{V_{cell}} \sum_{i=0}^{N_p} \frac{V_i \beta}{1-\varepsilon} \left(\vec{u}_g - \vec{v}_i \right) D\left(\vec{r} - \vec{r}_i \right) dV, \tag{3}$$

β is the interphase momentum transfer coefficient, calculated from the Ergun correlation for dense regimes ($\varepsilon < 0.8$) and Wen & Yu equation for gas volume fraction $\varepsilon \geq 0.8$. The motion of individual particles i in DEM is calculated using Newton's second law and the Euler equation, Eq. 4 and 5, respectively:

$$m_i \frac{d\vec{v}_i}{dt} = \frac{V_i \beta}{1-\varepsilon} \left(\vec{u}_g - \vec{v}_i \right) + m_i \vec{g} + \vec{F}_{SL} + \sum \vec{F}_{c,i} \tag{4}$$

$$I_i \frac{d\vec{\omega}_i}{dt} = \sum \vec{T}_i \tag{5}$$

On the right hand side of Eq. 4, forces determining the motion of particles are listed: drag force, Saffman lift (18), gravity as well as the particle-particle and particle-wall contact forces, respectively. The contact forces are modelled using a soft-sphere approach (19-22). The elastic normal and tangential contact forces are functions of the elastic and shear moduli, Poisson's ratios and the radii of contact partners. The inelastic energy adsorption is considered by damping forces, which are dependent on the restitution coefficients. The maximum tangential force is limited by the static friction. The rolling friction is included by a frictional torque. More details for the used model can be found in (6).
The pressure was recorded at 1000 Hz for 4.086 s in the simulations and for 8.192 s in the experiments. The shorter simulation period was used because the signal from simulation is more clean, compared to these from the experiments due to the absence of a sensor noise and the air fluctuations produced by the fan. Since the power of the FFT spectrum is a quadratic function of the data points' number in the input, the spectrum was normalized by dividing it by the square of the signal length, as proposed by Link *et al.* (11). The cells on both inlet areas were defined as two separate velocity inlets, the outlet zone on the top of the apparatus as a pressure outlet area with a gauge pressure of zero. Thus, the model represents rather a reactor operated using a compressed air. The apparatus introduced in (7) and the re-built apparatus are however operated in the sucking regime. In the experiments, the under-pressure above the particle bed and in the simulation the overpressure below the bed (in slits) were recorded (locations 1 and 2 in Fig. 1a, respectively).

RESULTS

In general, slot-rectangular spouted beds are reported to show a lower stability and a higher number of different flow regimes compared to the conventional axisymmetric ones (7,8,23,24). For the modeled apparatus, Gryczka *et al.* interpreted a single clean peak in the FFT spectrum of the pressure signal as an attribute of the stable operation of the modeled reactor and an occurrence of further peaks in the spectrum were attributed to instabilities (7). According to this finding, we modeled a stable and an instable regime at air flow rates 84 and 116 m^3/h, respectively. Figures 2 and 3 show the comparison of the instantaneous particle flow patterns captured from the experiments and the simulations in the time interval of 0.1s. The patterns of the granular flow and the bed expansion are predicted by the model quite accurately. The growing alternating deflection of the spout with increasing in the air flow rate is also predicted. The influence of the particles on the gas dynamics can be clearly seen in the pressure signal (Figures 3 and 5). Experimental measurements were performed at the established spouting; in the simulation the pressure was recorded from the process begin. Thus, the pressure drop shows the high initialization peak accompanying the breakthrough of the air through the fixed bed, a typical attribute of the spouted beds. The steady state conditions are achieved within 1.5-2 s, according to the evolution of the periodical pressure signal. The FFT-analysis was applied for the last 4.086 s of the simulation. The bed is spouted in a pulsating manner. The main frequency of the pressure fluctuations at air flow rate of 84 m^3/h is in the range of 6-7 Hz and is shifting at 116 m^3/h (main peak) to slightly higher frequencies. The discrepancy in the amplitudes of pressure drop are probably due to difference in the gas supply method and the different locations of pressure measurement. Some alternate spout deflection to the right and to the left, also reported in (7), can be recognized in figure 2. This spout deflection increases with the gas throughput und leads finally to an instable regime and an occurrence of additional peaks in the FFT frequency spectrum (7).

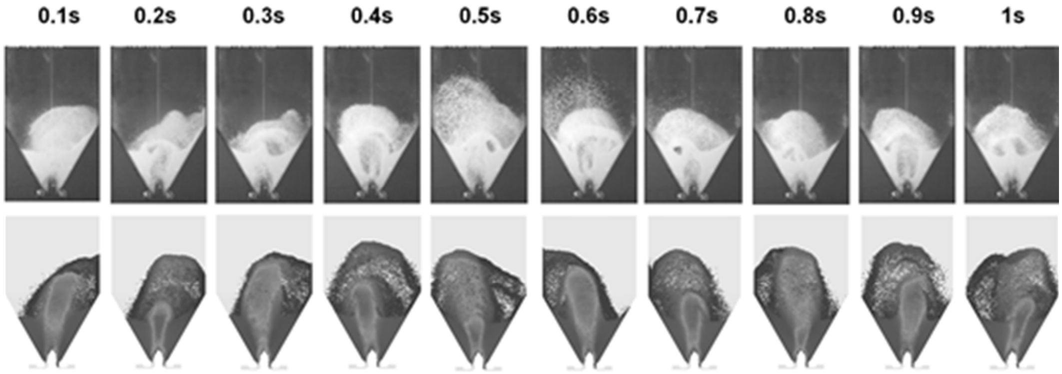

Figure 2: Instantaneous patterns of the stable granular flow at an air flow rate of 84 m^3/h; *top:* the experiment, *bottom:* the simulation.

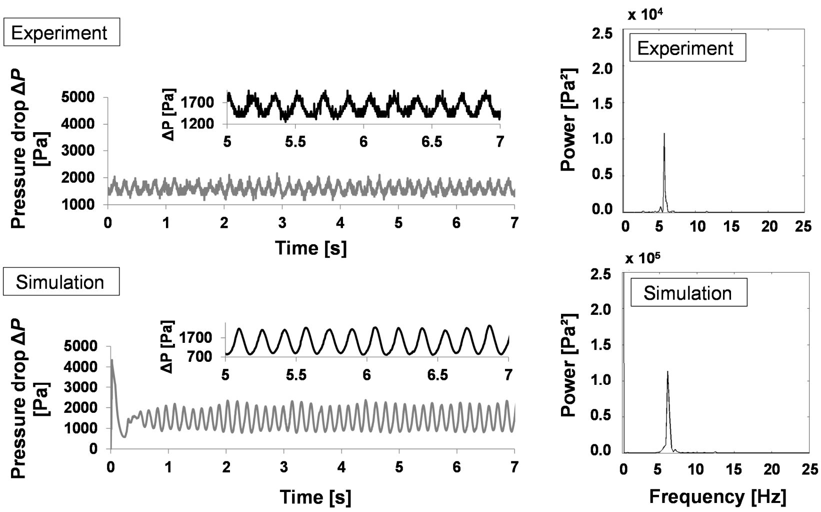

Figure 3: Fluctuations of pressure drop and the corresponding FFT-spectra obtained from the experiment and the simulation at an air flow rate of 84 m^3/h.

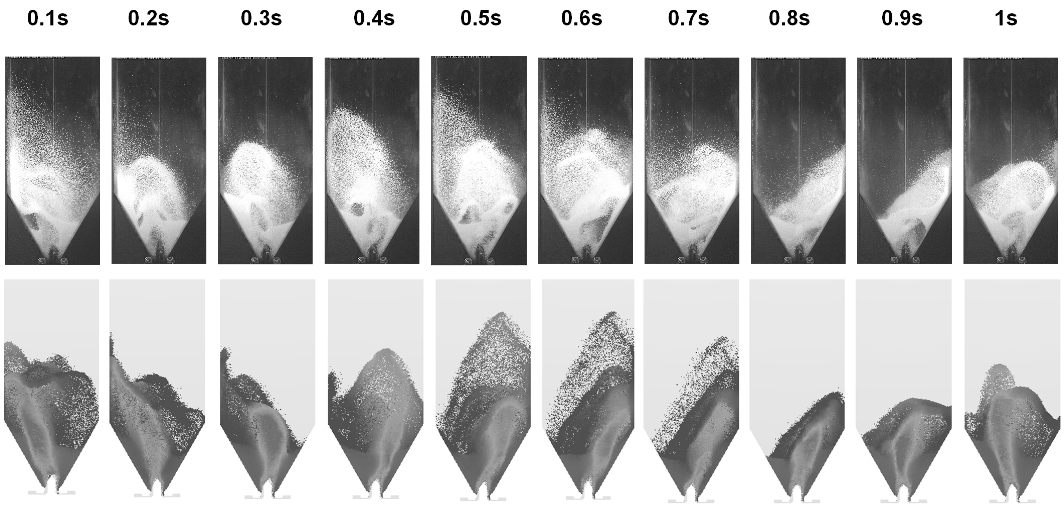

Figure 4: Instantaneous patterns of the unstable granular flow at an air flow rate of 116 m^3/h; top: the experiment, bottom: the simulation.

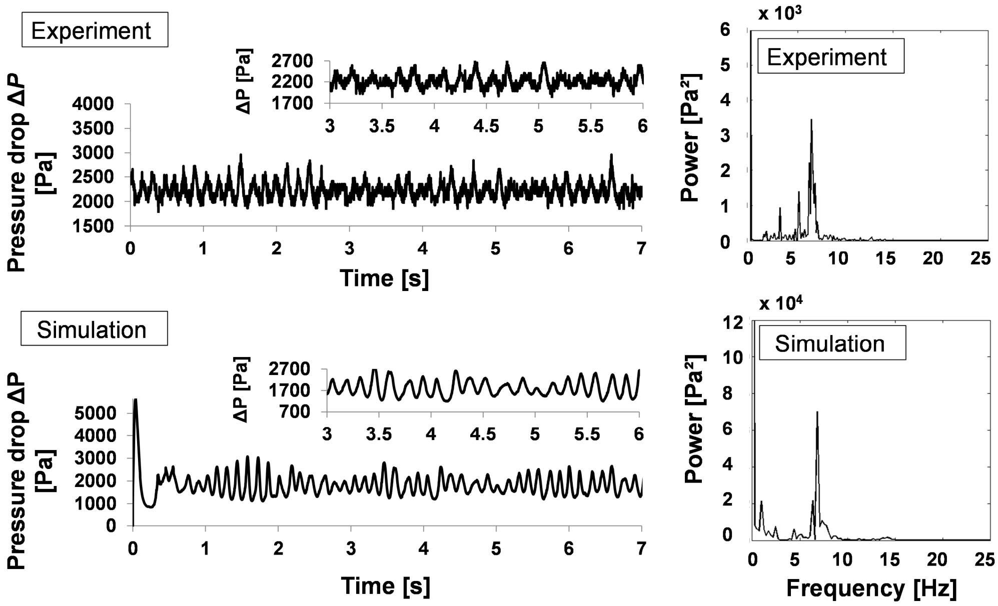

Figure 5: Fluctuations of pressure drop and the corresponding FFT-spectra obtained from the experiment and the simulation at an air flow rate of 116 m^3/h.

Figure 6 shows the vertical particle velocity in dependence on the apparatus thickness, averaged over the period after the decay of startup effects. One can see two areas of increased particle velocity in the vicinity of vertical walls (at y = 0 and 100 mm), also observed experimentally for the slot-rectangular spouted beds under similar conditions ("dense" spouting) and termed by Freitas *et al.* (24) and Chen (8) as "multiple spouts".

CONCLUSIONS

In this contribution spouting was simulated by using Discrete Particle Model. The characteristic periodical pressure fluctuations were predicted by the model. The particle flow patterns, bed expansion (height) and the transition stable spouting-instable regime were also predicted accurately. The transition can be recognized by using the FFT analysis both in the experiment and in the simulation.

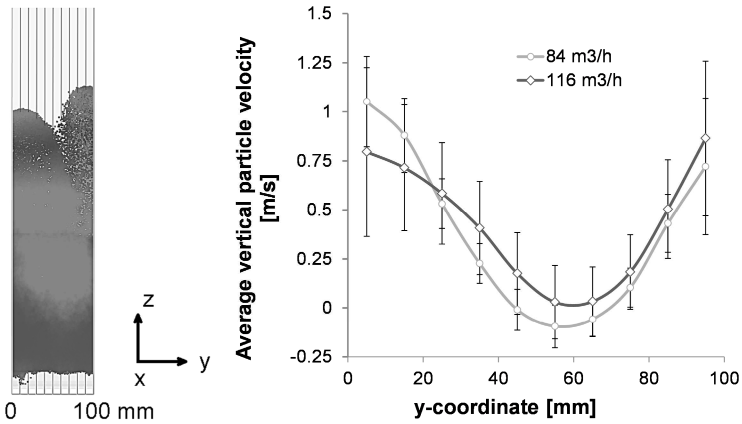

Figure 6: Time-averaged vertical particle velocity in spout in the direction of the apparatus thickness (y-direction).

ACKNOWLEDGEMENTS

We gratefully acknowledge for the financial support: Technology Foundation STW, The Netherlands and Deutsche Forschungsgemeinschaft (DFG), Germany. Project number HE 4526/5-1.

NOTATION

$\vec{g}$	Gravitational acceleration, m/s^2
I	Moment of inertia, kg·m^2
p	Pressure, Pa
$\vec{r}$	Particle position, m
$\vec{S}_p$	Drag sink term, N/m^3
$\vec{T}$	Torque, N·m
$\vec{u}_g$	Gas velocity, m/s
V	Volume, m^3
$\vec{v}_p$	Particle velocity, m/s
β	Interphase momentum transfer coefficient, kg/(m^{3}s)
λ_g	Gas bulk viscosity, kg/(m·s)
μ_g	Dynamic viscosity of the gas phase, kg/(m·s)
$\vec{\vec{\tau}}_g$	Gas phase stress tensor, Pa
$\vec{\omega}$	Angular velocity, 1/s

REFERENCES

1. T. Kawaguchi, M. Sakamoto, T. Tanaka, and Y. Tsuji. Quasi-three-dimensional numerical simulation of spouted bed in cylinder. *Powder Technol.,* 109 (2000), 3.
2. S. Takeushi, S. Wang, and M. Rhodes. Discrete element simulation of a flat-bottomed spouted bed in the 3-D cylindrical coordinate system. *Chem. Eng. Sci.*, 59 (2004), 3495.
3. X.-L. Zhao, S.-Q. Li, G.-Q. Liu, Q. Yao, and J.S. Marshall. DEM simulation of the particle dynamics in two-dimensional spouted beds. *Powder Technol*., 184 (2008), 205.
4. T. Swasdisevi, W. Tanthapanichakoon, T. Charinpanitkul, T. Kawaguchi, T. Tanaka, and Y. Tsuji. Investigation of fluid and coarse-particle dynamics in a two-dimensional spouted bed. *Chem. Eng. Technol.*, 27(2004), 971.
5. S. Limtrakul, A. Boonsrirat, and T. Vatanatham. DEM modeling and simulation of a catalytic gas-solid fluidized bed reactor: A spouted bed as a case study. *Chem. Eng. Sci.*, 59 (2004), 5225.

6. V. Salikov, S. Antonyuk, and S. Heinrich. Using DPM on the way to tailored prismatic spouted beds. *Chem. Ing. Tech.*, 84 (2012), 388.
7. O. Gryczka, S. Heinrich, V. Miteva, N.G. Deen, J.A.M. Kuipers, M. Jacob, and L. Mörl. Characterization of the pneumatic behavior of a novel spouted bed apparatus with two adjustable gas inlets. *Chem. Eng. Sci.*, 63 (2008), 791.
8. Z. Chen. Hydrodynamics, Stability and Scale-Up of Slot-Rectangular Spouted Beds. PHD thesis, *The University of British Columbia*, (2008), Vancouver.
9. L.A.P. Freitas, O.M. Dogan, C.J. Lim, J.R. Grace, and D. Bai. Identification of Flow Regimes in Slot-Rectangular Spouted Beds using Pressure Fluctuations. *Can. J. Chem. Eng.* (2004), 82, 60.
10. X. Bao, W. Du, and J. Xu. Computational Fluid Dynamic Modeling of Spouted Beds. In Spouted and spout-fluid beds (Eds: N. Epstein, J. R. Grace), *Cambridge University Press*, (2011), Cambridge.
11. J.M. Link, L.A. Cuypers, N.G. Deen, and J.A.M. Kuipers. Flow regimes in a spout-fluid bed: A combined experimental and simulation study. *Chem. Eng. Sci.*, 60 (2005), 3425.
12. V. Yakhot and S. A. Orszag. Renormalization Group Analysis of Turbulence. I. Basic Theory. *J. Sci. Comput*. 1 (1986).
13. O. Gryczka, S. Heinrich, N.G. Deen, M. van Sint Annaland, J.A.M. Kuipers, M. Jacob, and L. Mörl. Characterization and CFD-modeling of the hydrodynamics of a prismatic spouted bed apparatus. *Chem. Eng. Sci.* (2009), 64, 3352.
14. O. Gryczka, S. Heinrich, N. G. Deen, J. A. M. Kuipers, and L. Mörl. Three-Dimensional Computational Fluid Dynamics Modeling of a Prismatic Spouted Bed. *Chem. Eng. Technol*. (2009), 32, 470.
15. Ergun, S. Fluid flow through packed columns, *Chem. Eng. Prog.* (1952), 48, 89.
16. Y.C. Wen and Y.H. Yu, Mechanics of fluidization, *Chem. Eng. Prog. Symp. Ser.* (1966), 62, 100.
17. D. Gidaspow. Multiphase Flow and Fluidization. *Academic Press* (1994), San Diego.
18. P.G. Saffman. The Lift on a Small Sphere in a Slow Shear Flow. *J. Fluid Mech.* 22 (1965), 385.
19. H. Hertz. Über die Berührung fester elastischer Körper. *J. Reine Angew. Math.* (1882), 92, 156.
20. R. D. Mindlin. Compliance of Elastic Bodies in Contact. *ASME J. Appl. Mech.* (1949), 16, 259.
21. P.A. Cundall and O.D.L. Strack. A discrete numerical model for granular assemblies. *Geotechnique* (1979), 29, 47.
22. Y. Tsuji, T. Tanaka, and T. Ishida. Lagrangian numerical simulation of plug flow of cohesionless particles in a horizontal pipe. *Powder Technol.* (1992), 7, 239.
23. O.M. Dogan, L.A.P. Freitas, C.J. Lim, J.R. Grace, and B. Luo. Hydrodynamics and Stability of Slot-rectangular Spouted Beds. Part I: Thin bed. *Chem. Eng. Comm.* (2000), 181, 225.
24. L.A.P. Freitas, O.M. Dogan, C.J. Lim, J.R. Grace, and B. Luo: Hydrodynamics and Stability of Slot-rectangular Spouted Beds part II: Increasing Bed Thickness, *Chem. Eng. Comm.* (2000), 181, 243-258.